FEMS Microbiology Letters, 2023, **370**, 1–11
DOI: 10.1093/femsle/fnad027
Advance access publication date: 7 April 2023
Research Letter – Biotechnology & Synthetic Biology

An engineered *Escherichia coli* Nissle 1917 increase the production of indole lactic acid in the gut

Chrysoula Dimopoulou[1], Mareike Bongers[2], Mikael Pedersen[1], Martin I. Bahl[1], Morten O. A. Sommer[2], Martin F. Laursen[1], Tine R. Licht[1,*]

[1]National Food Institute, Technical University of Denmark, Kemitorvet, Building 202, DK-2800 Kgs. Lyngby, Denmark
[2]The Novo Nordisk Foundation Center for Biosustainability, Technical University of Denmark, Kemitorvet, Building 220, DK-2800 Kgs. Lyngby, Denmark
*Corresponding author. National Food Institute, Technical University of Denmark, Building 202, DK-2800 Kgs. Lyngby, Denmark. Tel: +45 35887186; E-mail: trli@food.dtu.dk
Editor: [Akihito Endo]

Abstract

The expanding knowledge of the health impacts of the metabolic activities of the gut microbiota reinforces the current interest in engineered probiotics. Tryptophan metabolites, in particular indole lactic acid (ILA), are attractive candidates as potential therapeutic agents. ILA is a promising compound with multiple beneficial effects, including amelioration colitis in rodent models of necrotizing enterocolitis, as well as improved infant immune system maturation. In this work, we engineered and characterized *in vitro* and *in vivo* an *Escherichia coli* Nissle 1917 strain that produces ILA. The 2-step metabolic pathway comprises aminotransferases native of *E. coli* and a dehydrogenase introduced from *Bifidobacterium longum* subspecies *infantis*. Our results show a robust engineered probiotic that produces 73.4 ± 47.2 nmol and 149 ± 123.6 nmol of ILA per gram of fecal and cecal matter, respectively, three days after colonization in a mouse model. In addition, hereby is reported an engineered-probiotic-related increase of ILA in the systemic circulation of the treated mice. This strain serves as proof of concept for the transfer of capacity to produce ILA *in vivo* and as ILA emerges as a potent microbial metabolite against gastrointestinal inflammation, further development of this strain offers efficient options for ILA-focused therapeutic interventions *in situ*.

Keywords: *E. coli*, indole lactic acid, lactate dehydrogenase, mouse study, engineered microbes, microbial therapeutics

Introduction

As a part of human physiology, the gut microbiome consists of millions of microbial species, which collectively function as an additional endocrine organ (Clarke et al. 2014). The vast array of microbially derived molecules in the gut influences the host in multiple ways, and microbiome imbalances have been linked to conditions like metabolic syndrome (Cani 2019), immune system maturation (Francino 2014), obesity (Sharma et al. 2018), inflammatory bowel diseases (IBD) (Lavelle and Sokol 2020), and neuropsychiatric conditions (Rutsch et al. 2020). Because of their multiple physiological connections in health and disease, these gut metabolites present an opportunity for developing a new generation of therapeutics; the a dvanced microbial therapeutics (AMTs), which are live biotherapeutic probiotics engineered for *in situ* therapeutic activity (Mimee et al. 2016).

Advances in synthetic biology allow the development of probiotic strains engineered to encode for desirable molecules and functions (Pedrolli et al. 2019). AMTs can be chosen or designed to survive the gastric environment and establish themselves in the intestine. *In situ* delivery of AMT-produced molecules is beneficial since loss resulting from the gastric passage can be avoided, and local dosing is expected to increase the therapeutic effect. In addition, genetic manipulation may further expand their capabilities in multiple ways, such as controlling the AMTs exact localization (Ryan et al. 2009), expressing the therapeutic molecule on demand (Kotula et al. 2014), and controlling the colonization period (Shepherd et al. 2018) as reviewed elsewhere (Ozdemir et al. 2018).

A promising approach in engineered probiotics comprises the application of AMTs that will enhance the production of beneficial metabolites native to the microbiome (Suez and Elinav 2017, Singh et al. 2019, Lavelle and Sokol 2020, Peredo-Lovillo et al. 2020). Natural producers, i.e. probiotic strains, are not always colonizing efficiently (Zmora et al. 2018, Han et al. 2021) and the lack of information on their exact interactions with the microbiome obstructs efforts of standardized use. Moreover, as these compounds are mainly secondary metabolites, their production is greatly influenced by the surrounding microbial community (Chevrette et al. 2022). Incorporation of new biosynthetic pathways into AMTs offer the opportunity of effective options for control of the production of desired metabolites, and provide new opportunities for localization and colonization of the producing strain in the gut. Application of AMTs is thus relevant in contexts where the natural producers in the microbiome are low or depleted, for example due to antibiotic treatments or disease-induced alterations of the microbiome composition.

Indole lactic acid (ILA) is such a metabolite, as evidence suggests that ILA, besides acting directly as an antimicrobial (Zhou et al. 2022) promotes immune system (Henrick et al. 2021, Laursen et al. 2021) and neuronal (Wong et al. 2020) development and attenuates inflammation in the infant and adult gut (Ehrlich et al. 2020, Meng et al. 2020). Its production is a result of tryptophan fermentation occurring in a two-step reaction. First, an aromatic aminotransferase converts tryptophan to indole pyruvic acid (IPyA), and an aromatic lactate dehydrogenase further converts IPyA to ILA.

Received: January 13, 2023. **Revised:** March 27, 2023. **Accepted:** March 31, 2023

This reaction is part of a longer pathway with indole propionic acid (IPA) as its end product (Liu et al. 2020). ILA-producing intestinal bacteria encode either for a complete pathway or parts of it (Roager and Licht 2018), and the enzymes involved in these pathways are believed to be able to catalyze the conversions of all three aromatic amino acids (Dodd et al. 2017). Multiple gut species are ILA producers, amongst them *Bacteroides*, *Clostridium*, *Peptostreptococcus* (Russell et al. 2013), *Lactobacillus* (Cervantes-Barragan et al. 2017), and *Bifidobacterium* (Sakurai et al. 2019) species.

Modern day diets have been shown to further decrease the microbiome ILA producers (Wilck et al. 2017). Producing *Bifidobacterium* sp. are unpredictable colonizers (Xiao et al. 2021, Derrien et al. 2022), and the use of engineered strains allows for utilization of genetic tools that enhance strain engraftment. Such tools have already been developed for use in *Escherichia coli* Nissle (EcN) (Kearney et al. 2018, Shepherd et al. 2018). Additionally, EcN offers multiple possibilities to ensure biocontainment of engineered strains (Mandell et al. 2015, Piraner et al. 2017). We therefore aimed to develop an EcN strain that boosted ILA production *in vivo* and could serve as a proof of concept inspiring further development. A gene encoding the aromatic lactate dehydrogenase, which is exogenous to EcN, was introduced on a modified native plasmid of EcN, and the capacity of the strain to produce ILA was tested *in vitro* and *in vivo* in a mouse model. The genetic construct was designed to constitutively produce higher levels of ILA than obtained with naturally producing *Bifidobacterium* sp. (Sakurai et al. 2019). In addition to the production of ILA, we monitored the aromatic lactic acids (aLAs) derived from tyrosine and phenylalanine, as well as the precursor aromatic amino acids and the intermediate aromatic PyAs.

Materials and methods

Strains

The probiotic strain used in this study, EcN_GFP, StrepR: *E. coli* Nissle 1917 is a modified version of the wild-type *E. coli* Nissle 1917 (tradename Mutaflor, Ardeypharm, Germany). It expresses GFP (integrated into the Tn7 attachment site) and encodes for streptomycin resistance. In the following, this strain will be noted as EcN, while the wild-type strain will be noted as EcN WT. All cloning procedures were performed in *E. coli* TOP10 (Invitrogen, USA), except for the final transformation step where the plasmids were introduced into the EcN strain. EcN electrocompetent cells were created using standard protocols (Green et al. 2012). All bacterial cultures grew in LB media and were incubated at 37°C with vigorous shaking. When appropriate, media were supplemented with 30 μg/ml Kanamycin and/or 50 μg/ml streptomycin for antibiotic selection. Anaerobic cultivations were conducted in an anaerobic work station Whitley A95 (Don Whitley Scientific Limited, UK) with an atmosphere of 10% H_2, 10% CO_2, and 80% N_2.

Plasmids

The *aldh* gene (GenBank accession no. WP_014484799.1) was amplified from *Bifidobacterium longum* subsp. *infantis* (DSM 20088), with primers aldh_F: GTGTATAATTGGTTACTCATAGACATAGAAGGGAAAAAGTAATGGTCACTATGAACCGC and aldh_R: GTAAACTTGGTCTGACAGTCACAGCAGCCCCTTGC), which included a 15–18bp-long sequence of the vector on their 5′end (underlined). An RBS appropriate for *E. coli* Nissle 1917 was generated *in silico* with a target initiation rate of 10 000 au (Salis 2011, Hecht et al. 2017), and its sequence was integrated into the 5′end of aldh_F alongside an appropriate promoter sequence (underlined). The promoter used in this study was #1.7 of the Schantzetta library of constitutive promoters specifically developed for precision engineering in AMT development (Armetta et al. 2021) Primers pHH_F: CACTGCAAGGGGCTGCTGTGACTGTCAGACCAAGTTTACTATACTTTAGGCTGCCAGTCG and pHH_R: CTATGAGTAACCAATTATACACGTAGGAGGAACGACGAGTCAAGCAGAGGTACCGCGGACAAGAC were used for the amplification of the pHH vector. The primers included a part of the promoter and RBS (pHH_R) and the *aldh* sequence (pHH_R) on their 5′end (underlined). Cloning was performed with the Gibson assembly method (NEB, USA). The pHH-control plasmid was generated by amplifying the pHH backbone with primers pHH_bck_F: TATACTTTAGGCTGCCAGTC and pHH_bck_R: CCAATTATACACGTAGGAGG and then performing a blunt ligation of the product. Both plasmids were introduced in the EcN strain by standard electroporation, creating EcN *aldh* and EcN strains.

In vitro characterization of the engineered strain

Growth curves were generated from single colonies overnight (ON) inoculates, that next day were diluted 1:1000 in fresh medium and incubated at 37°C for 10 hours in microplate readers Victor X4 (Perkin Elmers, USA) in aerobic conditions and Inifinite F50 (Tecan, Switzerland) in anaerobic conditions. OD_{600} measurements were taken every 30 minutes following a shaking pulse.

Single colonies of the strains were inoculated ON and next day, were diluted 1:50 in fresh medium and incubated to an OD_{600} of around 0.4. OD (early logarithmic phase, time = 0 hour) was measured with Novaspec® III + Spectrophotometer (Biochrom, UK). After 2 hours of incubation, the strains were tested for ILA production by LC–MS as described below. Samples were taken at 0 hours and 2 hours, centrifuged at 16 000 *g* for 10 minutes at 4°C, and the supernatant was collected and stored at −20°C for metabolite profiling. The 2-hour incubation was performed in triplicates. The experiment was repeated three times. The total protein content of the samples at 0 hours was used to normalize the metabolite concentrations detected in the 2 hours samples. The total protein content was quantified using Pierce BCA Protein Assay kit (Thermo Scientific, USA).

Strain preparation for oral dosing—flow cytometry

EcN *aldh* and EcN strains were grown ON. The next day, the cultures were centrifuged at 4000 *g* for 10 minutes and washed two times with sterile PBS. Bacteria were re-suspended in sterile PBS. Both strains continuously produce GFP; thus absolute measurements of their concentration were obtained by flow cytometry, using flow cytometer MACSQuant® VYB and software MACSQuantify™ (Miltenyi Biotec, Germany). Following absolute quantification, the concentration of the PBS suspensions was adjusted to 10^8 CFU ml^{-1} and the solutions were stored at room temperature until oral gavage.

In vivo experiment

NMRI mice (n = 16, 6-weeks old) were purchased from Taconic Biosciences (Lille Skensved, Denmark). Throughout the experiment, they were housed under controlled environmental conditions (12-h light/dark cycles, temperature 22°C, humidity 55%, 50 air changes per hour) and had access to ad libitum water and food (SAFE Scientific Diet A30). During the first week, they were randomly housed in pairs for acclimatization.

On the first day of treatment, we allocated the mice into two groups of eight (each group housed into four cages of two animals) and their drinking water was supplemented with streptomycin sulfate (5 g l^{-1}). The solution was sterile filtered (Bottle Top Vacuum Filter with 0.22 μm pores) and stored at 4°C until use. The assignment to groups was randomized per weight. The next day, the mice were gavaged with bacterial solutions of the engineered strains (100 ml of a solution with 10^8 CFUs/ml). One group received the EcN *aldh*, and the other the EcN strain. Three days after, the animals were anesthetized in hypnorm/midazolam (0.1 ml/10 g SC) before opening the abdominal cavity/thorax and withdrawal of heart blood (collected in sterile Eppendorf tubes) and euthanasia by cervical dislocation.

Animal weight was recorded on the first and last day of the intervention. The Danish Animal Experiments Inspectorate approved the experimental design and protocol with authorization number 2020–15-0201–00484 C1. The National Food Institute in-house 'Animal Welfare Committee for animal care and use' oversaw the experiments.

Collection of samples: Fecal samples were collected daily from each individual mouse from one day before streptomycin administration. Each pellet was stored at −80°C within 30 minutes after collection. Peripheral blood was sampled on the day of streptomycin treatment and before termination of the animals and stored at −20° until further processing. At the time of dissection, gut content (from the ileum, cecum, and colon) samples were collected, temporarily stored at 4°C and then moved to −80°C until further processing.

CFU enumeration

Upon euthanization, fresh gut content samples from the ileum, cecum, and colon of each mouse were diluted in sterile MilliQ water in a ratio of 1:5 and vortexed until all content was dissolved. The samples were serially diluted in decimals of up to 10^{-9} and plated on LB plates supplemented with streptomycin that selects for the chassis strain regardless of pHH backbone, or a combination of streptomycin and kanamycin that select for the chassis and the pHH backbone. The dilutions ranging from 10^{-4} to 10^{-9} were plated in triplicates using the single plate-serial dilution spotting technique on 1-well culture plates (Thomas et al. 2015).

DNA extraction

On the day of DNA isolation, fecal and gut content samples were thawed at 4°C, sterile MilliQ water was added at a ratio of 1:5, followed by vortexing until all fecal matter was dissolved. Samples of <20 mg were diluted in 100 µl sterile MilliQ, and the dilution factor was calculated individually during downstream analysis. The mix was centrifuged for 10 minutes at 16 000 *g* at 4°C. The pellet was used for DNA extraction with the DNeasy PowerSoil Kit (Qiagen, Germany). DNA purity and concentration were assessed with the Qubit dsDNA HS assay kit (Thermo Fisher Scientific, USA). The supernatants were transferred to new tubes, and were centrifuged under the same conditions and the subsequent supernatants were transferred in new tubes and stored at −20°C until further processing.

Quantitative PCR

Strain colonization was assessed by absolute quantification using qPCR on the fecal and gut content DNA samples. The assay was performed using the LightCycler® 480 SYBR Green I Master Mix (Roche, Switzerland) with strain-specific primers. Forward primer 453: 5′-TCTTCACCTCGAGTTTACACC-3′ binds to genomic DNA 25 bps upstream of the GFP insertion site and Reverse primer 13: 5′-CTTTTCACTGGAGTTGTCCC-3′ binds 10 bp downstream of the GFP insertion site. A total of 5–20 ng of total DNA were used as a template and the reaction volume was 10 µl. Each reaction ran in triplicates in a 384-well format on the LightCycler® 480 Instrument II (Roche, Switzerland). The program comprised 5 minutes at 95°C, followed by 42 cycles of 10 seconds at 95°C, 15 seconds at 52°C and 15 seconds at 72°C. Melt curve analysis comprised 5 minutes at 95°C, 1 minute at 65°C and continuous temperature increase (ramp rate 0.11°C s–1) until 98°C. The standard curve was prepared from tenfold dilutions of the EcN DNA at a range of 10^0 to 10^7 copies/µl. Replicates with SD of Ct values >0.5 were excluded from further analysis. Data analysis was performed with the LinRegPCR software (Ruijter et al. 2009).

Quantification of aromatic amino acids and metabolites by LC–HRMS

Standard solutions of the nine analytes and three internal standards solutions (IS) were prepared to a final concentration of 1 mg/ml, as noted in Supplementary Table 1. An IS mix solution (16 µg/ml) was prepared in MilliQ water, containing all three isotope standards, and a standard mix solution (40 µg/ml) containing all aromatic amino acids and metabolites. The solutions were then combined and mixed with MilliQ water to reach final concentrations of 0.1 µg/ml, 0.5 µg/ml, 1 µg/ml, 2 µg/ml, 4 µg/ml, 10 µg/ml, and 20 µg/ml of the standard analytes and 4 µg/ml of the IS. Calibration curves were calculated from the analysis of the aforementioned standard mixes. Preparation of the fecal and gut content samples was performed with acetonitrile as the protein precipitation agent, following a previously described protocol (Nielsen et al. 2018). The IS mix solution was added to an optimized final concentration of 4 µg/ml. Serum samples were processed as described by Zhu and colleagues (Zhu et al. 2011). All LC vials and was stored at −20°C until analysis.

Statistical analysis

Statistical analysis was performed with the GraphPad Prism software, version 9 (GraphPad Software Inc., USA). Results are expressed as mean and standard deviation (SD) in the bar plots or median and minimum/maximum values in the box plots. Normal distribution of the variables was assessed with the Kolmogorov–Smirnov test ($P > 0.05$). Outliers were identified and subsequently removed by application of the ROUT method (Q = 1%). Data from the *in vitro* experiments was analyzed with multiple unpaired *t*-tests with Welch's correction. Two-way repeated measures ANOVA tests and the uncorrected Fisher's LSD test was used for analyzing data from the *in vivo* experiments and in cases of missing data, the mixed model was used instead. In LC–HRMS data analysis, values were below the limit of quantification (LOQ) and above the limit of detection of the method were replaced with the appropriate LOQ/2 value. A *P*-value of <0.05 was considered significant. Correlation analysis was performed by the use of Spearman's rank test and to account for multiple testing, the method for controlling false discovery rate (FDR) developed by Benjamini and Hochberg was applied ($q > 0.05$) (Benjamini and Hochberg 2000).

Results

Construction of EcN *aldh*

Escherichia coli Nissle 1917 (EcN) has the ability to produce IPyA endogenously (Smith and Macfarlane 1996, Romasi and Lee

2013). Thus our objective was to introduce a lactate dehydrogenase (Aldh) originating from *Bifidobacterium longum* subsp. *infantis*, which converts IPyA to ILA (Laursen et al. 2021). Tryptophan is converted to ILA through IPyA (Fig. 1A), and phenylalanine and tyrosine are converted to phenyllactic acid (PLA) and 4-hydroxyphenyllactic acid (4HPLA) through phenyl pyruvic acid (PPyA) and 4-hydroxy-phenyllpyruvic acid (4HPPyA) (Fig. 1B). The *aldh* gene was cloned downstream of a constitutive promoter on a modified version of one of the cryptic plasmids of EcN. In aerobic cultures of TOP10 *E.coli* strain transformants, ILA, PLA, and 4HPLA all reached high levels (Fig. 1C). Cultures of TOP10 *E.coli* bearing the empty vector did not produce any of the three aLAs, except for traces of PLA, verifying the contribution of Aldh in aLA production.

The engineered plasmids were transformed into our chassis EcN strain, creating EcN carrying the empty vector and EcN *aldh*, carrying the pHH-*aldh* vector, respectively. Grown in LB medium, the cultures did not exhibit any large growth differences during either aerobic or anaerobic cultivation (Supplementary Figs 1A and 1B).

Under aerobic conditions, the ILA levels of EcN *aldh* cultures were significantly higher than in the respective cultures of EcN, which did not produce ILA above the quantification level (Fig. 1D). Anaerobic conditions provided similar results (Fig. 1E). ILA was almost absent from the EcN cultures; thus, all ILA detected in the EcN *aldh* cultures could be attributed to the introduced Aldh catalyzing the conversion of IPyA. PLA and 4HPLA were also detected in significantly high amounts in the EcN *aldh* cultures. However, in contrast to the ILA yield, PLA, and 4HPLA reached consistently lower concentrations under aerobic condition, suggesting favourable metabolic conditions in the absence of oxygen (Fig. 1E).

To further study the characteristics of the strains, we measured the concentration of tryptophan, phenylalanine and tyrosine and their respective pyruvic acids in the cultures. As, LB is a rich medium, no additional aromatic amino acids were supplemented. Their concentrations at early logarithmic phase are noted in Supplementary Table 2. All tryptophan and approximately a tenth of phenylalanine and tyrosine were consumed in the EcN *aldh* aerobic cultures. Under anaerobic conditions, the consumption of aromatic amino acids was reduced, most likely due to the slower growth exhibited by the strains. Compared to the EcN strain, EcN *aldh* consumed similar levels of the available aromatic amino acids, indicating a redirection of tryptophan consumption towards ILA production (Supplementary Table 2). Since its growth was unaltered, this redirection potentially did not cause any considerable disturbance of the EcN's innate metabolism. The intermediates to the pathway, IPyA and 4HPPyA, were detected only in traces, except for PPyA, which reached quantifiable amounts in the EcN *aldh* strain (Supplementary Table 2).

In vivo experiment and streptomycin model

We evaluated the capacity of the strains to generate ILA *in vivo* by utilizing a mouse colonization model. EcN is a transient colonizer of the murine intestinal tract (Conlan et al. 2001), thus we applied the widely used streptomycin-treated mouse model to ensure colonization (Wadolkowski et al. 1988). Streptomycin reduced the intestinal colonization barrier and selected for the resistant EcN *aldh* and EcN strains. Conventional NMRI mice ($N = 8$ per group) received streptomycin in the drinking water one day prior to oral administration with EcN or EcN *aldh*. We measured the fecal concentration of the relevant metabolites before and after streptomycin treatment to reveal the effects of the antibiotic on ILA production by the indigenous microbiota, as well as the concentration of the metabolites in feces for three days following the oral administration with the EcN strains.

In the pristine mouse microbiome, PLA was present in high concentrations compared to the much lower levels of 4HPLA and ILA. Streptomycin treatment did not induce alterations to ILA levels (Fig. 2A), while it caused a significant reduction of PLA and 4HPLA concentrations (Fig. 2B and C). Despite their mainly dietary origin, phenylalanine and tyrosine concentrations were decreased by streptomycin treatment, implying a substantial microbial supplementation of those amino acids in the microbiome aromatic amino acid pool, while tryptophan concentration was unaffected by streptomycin treatment (Supplementary Fig. 2A).The intermediate aPyAs were either not detected of detected in concentrations below to the limit of quantification before as well as after streptomycin treatment (Supplementary Fig. 2B), with the exception of PPyA.

Bodyweight measurements were recorded on the first and last days of the experiment. Colonization with the strains did not affect the weight, consistent with reports that EcN is nontoxic for mice (Sonnenborn and Schulze 2009) (Supplementary Fig. 3). As assessed by qPCR, the EcN, and EcN *aldh* strains reached similar levels in feces and gut samples (Fig. 2D and E). The results were confirmed by enumerating of CFUs on selective agar (Supplementary Fig. 4A). Absence of plasmid loss was verified by plating of gut content on appropriate selective plates (Supplementary Fig. 4B).

EcN *aldh* increases aLAs *in vivo*

The ability of the engineered strain to produce ILA *in vivo* was assessed by measurement of its concentration in fecal and gut content samples. Administration of EcN *aldh* led to a considerable yield of ILA in the feces of the mice, reaching a 3-day median average of 58.2 ± 13.3 nmol/g (Fig. 3A), 3.6-fold higher than the control group. Likewise, ILA levels were 5.5-fold and 4.6-fold higher in the cecum and colon of mice carrying the EcN *aldh* strain compared to mice carrying the control strain (Fig. 3A). While ILA concentration was similar across compartments in the EcN mice, in the cecum of EcN *aldh* mice, ILA was 149.03 ± 123.56 nmol/g, and only 64.97 ± 51.56 nmol/g was detected in the colon. PLA and 4HPLA followed a pattern similar to ILA, exhibiting fecal levels 3.5-fold and 3.6-fold higher in the EcN *aldh* mice than in the EcN mice. Analysis of the cecal and colonic gut contents confirmed their higher levels in animals colonized with EcN *aldh* (Fig. 3B and C).

Collectively, all aLAs rose in concentration after the oral gavage with either EcN or EcN *aldh*. However, PLA levels did not reach pre-strep levels in any of the two groups (Fig. 3B), while, in contrast, 4HPLA and ILA increased above pre-strep levels in both groups. ILA rose continuously in all animals, with the concentration in the EcN *aldh* group displaying the highest increase. Specifically, on day three, the ILA concentration of EcN *aldh* mice was on average 17.9(± 13.4)-fold higher than ILA concentration observed in the pristine microbiome of each mouse, whereas presence of EcN contributed to an ILA increase of an 11(± 13.6)-fold.

Influences on aromatic amino acids and metabolites

Since EcN *aldh* selectively catalyzes the conversion of the aromatic amino acids, tryptophan, phenylalanine, and tyrosine concentrations were measured to follow the impact of the process on the substrate concentrations in the gut. Likely due to the excess availability of peptides and amino acids in the intestinal environment, the aromatic amino acid concentrations were not significantly different between the two groups (Supplementary Fig. 5A and 5B).

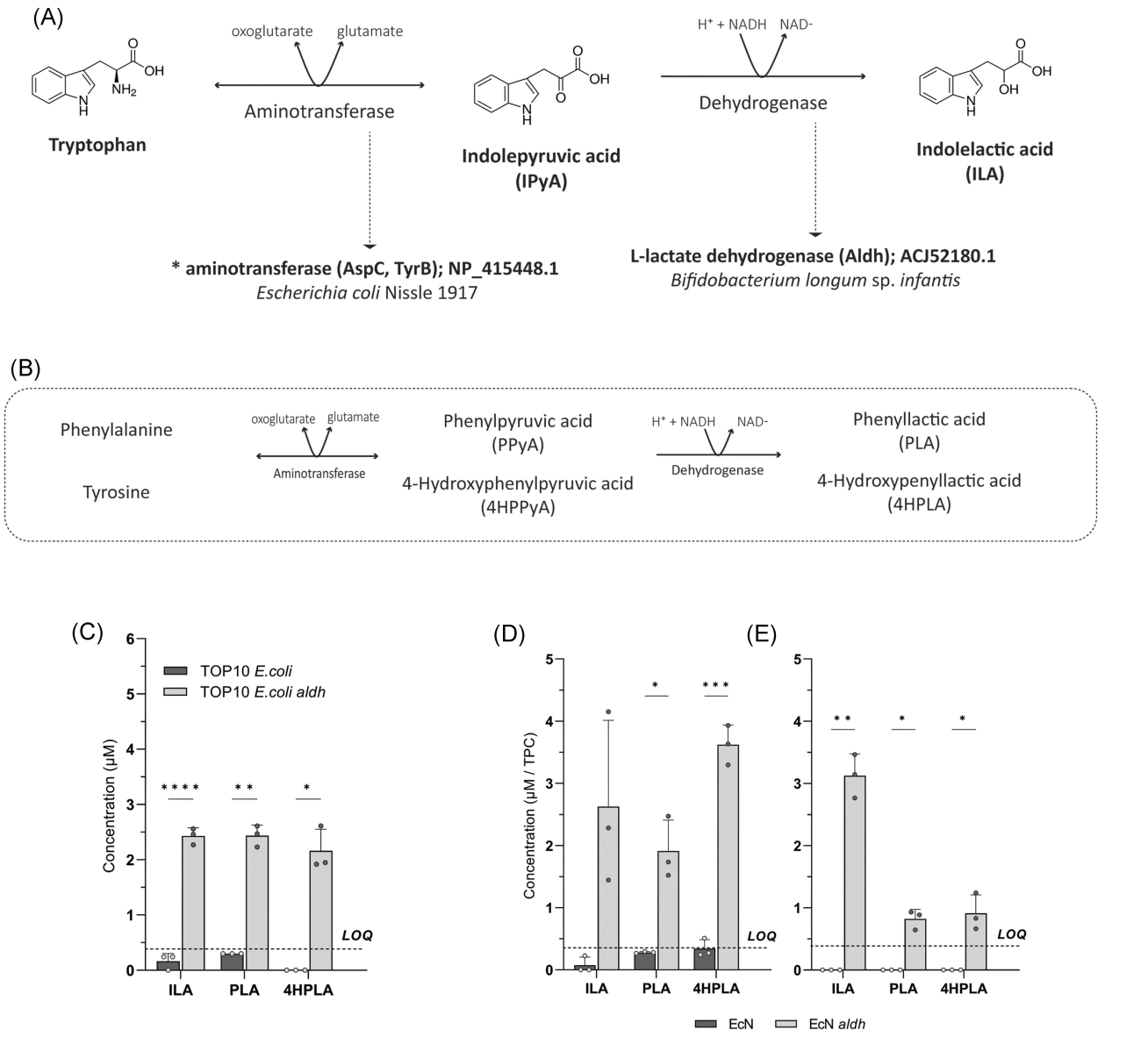

Figure 1. Development of an *E. coli* Nissle 1917 strain for ILA production (EcN *aldh*). (A) Tryptophan to ILA degradation pathway. An aminotransferase converts tryptophan to IPyA and a dehydrogenase converts IPyA acid to ILA. * Denotes putative endogenous enzymes that may contribute to the catalysis of the pathway in the EcN *aldh* strain. (B) Conversion of phenylalanine to PLA and tyrosine to 4HPLA by the same enzymes. (C) ILA, PLA, and 4HPLA concentration in spent media of TOP10 *E.coli* cultures. TOP10 *E.coli* is transformed with the pHH empty backbone. TOP10 *E.coli aldh* is transformed with the pHH-*aldh* construct. The mean and standard deviation (error bars) of technical triplicates are shown. (D and E) aLA concentrations per total protein content (TPC) in the engineered strain spent media under (D) aerobic and (E) anaerobic conditions. The mean and standard deviations (error bars) of three biological triplicates are shown. Dashed lines denote the limit of quantification of the method. Multiple unpaired *t*-tests with Welch correction, were performed to determine statistically significant differences. *$P < 0.05$, **$P < 0.01$, ***$P < 0.001$, ****$P < 0.0001$.

Compared to the pre-treatment levels, neither the EcN nor the EcN *aldh* exhibited drastic changes in their tryptophan levels, suggesting that the strains cause no major disturbance in tryptophan intestinal concentration. Measurement of the three intermediate aPyAs revealed that IPyA was present only in traces (data not shown). At the same time, PPyA and 4HPPyA reached much higher concentrations and was significantly higher in the EcN *aldh* group than in the EcN group (Supplementary Fig. 6).

Systemic circulation of the metabolites

Before strep treatment, the concentration of ILA in blood (serum) was on average 1.55 ± 0.24 μM, and PLA and 4HPLA reached concentrations of 1.1 ± 0.2 μM and 1.1 ± 0.4 μM, respectively. During AMTs colonization, ILA increased significantly in the group that received EcN *aldh*, whereas no significant increase of serum ILA was detected in the EcN group (Fig. 4A). The average fold change was 1.8 ± 0.4 and 1.2 ± 0.4 for the EcN *aldh* and the EcN groups, respectively, suggesting a causative role of the ILA-producing AMT in the observed increase also in circulation. PLA concentration in the serum was reduced compared to pre-strep treatment regardless of the strain (Fig. 4B), while serum 4HPLA was significantly affected only in the group that received the control strain (Fig. 4C). Both AMTs caused no major changes in the serum aromatic amino acids (Supplementary Fig. 7A). The aPyAs concentration did not change, except for an increase of 4HPPyA in the EcN animals (Supplementary Fig. 7B).

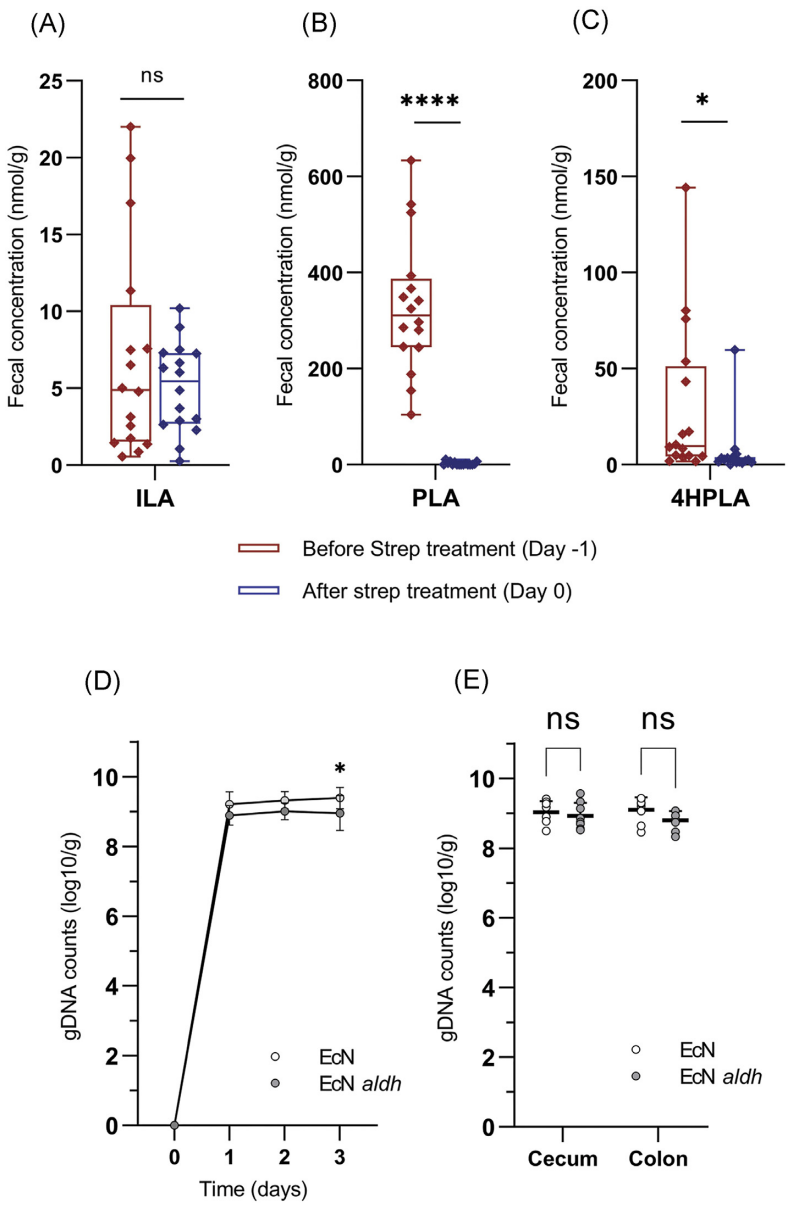

Figure 2. Streptomycin effect and AMTs colonization (A, B, and C). Fecal concentrations of ILA, PLA, and 4HPLA on the day before and the day of streptomycin treatment. The box plots depict the median and minimum and maximum measurements from all animals ($n = 16$). Statistical significance was calculated by two-tailed student *t*-test. (D and E) The engineered strains colonization numbers in fecal and gut content samples. The graphs represent the mean from eight mice and the error bars depict the standard deviation. Statistical analysis was performed using (A, B, C, and E) paired *t*-tests, and (D) two-way ANOVA, uncorrected Fisher's LSD. $^{*}P < 0.05$, $^{**}P < 0.01$, $^{***}P < 0.001$, $^{****}P < 0.0001$.

Correlation analysis between colonic AMT colonization and aromatic metabolites

The correlation between the colonic density of the AMTs and the detected metabolites in the fecal, colon, and serum samples on day 3 was examined by Spearman's rank analysis (Table 1). EcN *aldh* counts in colon correlated with ILA, PLA, and 4HPLA level in feces and with ILA and 4HPLA in the colon. Pearson's correlation analysis between EcN aldh colonic colonization and fecal and colonic ILA levels- suggested that the relationship between the AMT and its product is linear (data not shown). The aPyA levels in feces were also associated to EcN *aldh* density. In contrast, the aromatic amino acid levels in feces and colon were independent of the introduced strains in the colon, indicating that the presence of these strains did not significantly disturb the nutrients available to the endogenous microbiota. Similar analysis of the cecal density of the AMT in relation to the detected metabolites in the fecal, cecal, and serum samples on day 3 did not reveal significant correlations (data not shown).

Discussion

We have constructed an engineered probiotic, EcN *aldh*, which successfully produced ILA *in vitro* and *in vivo* in the mouse gut. The native probiotic strain of EcN 1917 encodes metabolic pathways capable of IPyA production. Thus, by adding a single gene encoding an enzyme that efficiently converts aPyAs to the corresponding aLAs to one of the cryptic plasmids of EcN, we successfully directed its metabolism towards ILA production. The engineered strain was functional under aerobic and anaerobic conditions and grew at the same rate as its unmodified counterpart. *In vivo*

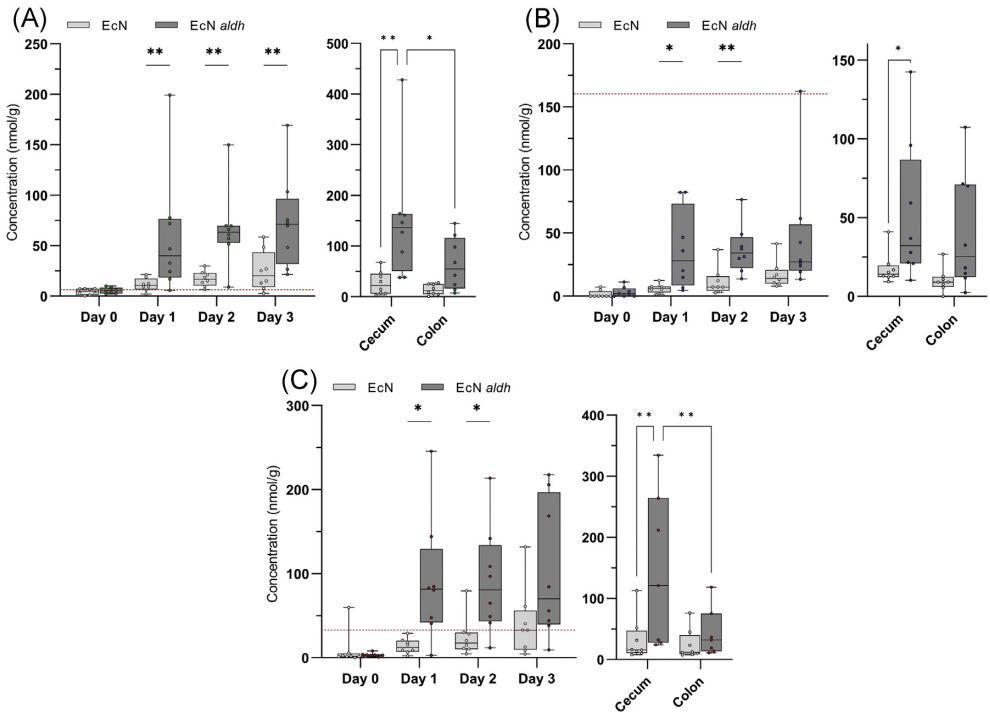

Figure 3. aLAs and aromatic amino acids in mice treated with EcN and EcN *aldh*. Concentration of (A) ILA, (B) PLA, and (C) 4HPLA in fecal and gut content samples of mice treated with the AMT strains. The red dotted line notes their average pre-streptomycin levels. Statistical significance was determined by repeated measures two-way ANOVA, Fisher's LSD test and two way ANOVA, Fisher's LSD test. All graphs illustrate the median, minimum, and maximum values from the independent biological replicates across the days of the experiment. * $P < 0.05$, ** $P < 0.01$, *** $P < 0.001$, **** $P < 0.0001$.

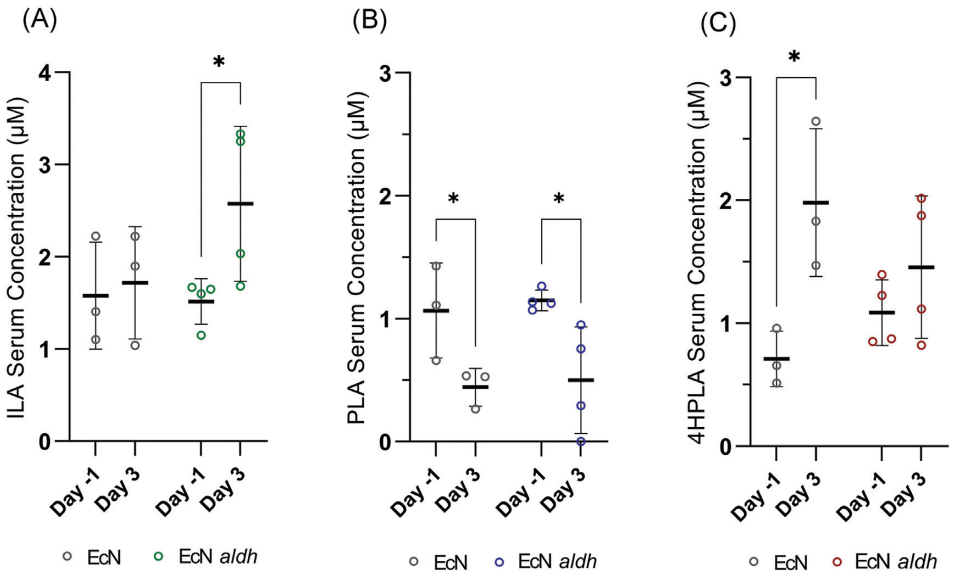

Figure 4. Blood pharmacokinetics of EcN *aldh* mice. (A) Serum concentration of (A) ILA, (B) PLA, and (C) 4HPLA before and after treatment with the AMT strains; all graphs plot the mean and standard deviation (error bars) of four independent biological replicates. Statistical significance was calculated by paired values, mixed-effects analysis, Fisher's LSD test; *$P < 0.05$, **$P < 0.01$, ***$P < 0.001$, ****$P < 0.0001$.

analysis of EcN *aldh* displayed a promising candidate for future use as an AMT. All aLAs were increased in the fecal content of the treated mice, while no pronounced effects on the initial concentrations of the aromatic amino acids were detected. Additionally, colonization by the engineered strain resulted in a detectable rise of ILA in the serum of the animals, while the unmodified EcN did not produce the same effect.

EcN 1917 was chosen as the chassis strain due to its ease of genetic manipulation (Schröder et al. 2022) and the health benefits associated with its probiotic nature (Ou et al. 2016). The wide use of this strain ensures a body of valuable knowledge regarding safety assessment in connection to putative future clinical trials. In contrast to other *E.coli* vectors (Lin-Chao and Bremer 1986, Diaz Ricci and Hernández 2000, Wang et al. 2006), the cryptic plasmids

Table 1. Correlation analysis of the relationship between the qPCR-assessed EcN and EcN *aldh* colonic levels and the measured aLAs and aPyAs in the fecal, colon, and serum samples on day 3.

	Fecal content		Colon content		Serum	
	EcN	EcN *aldh*	EcN	EcN *aldh*	EcN	EcN *aldh*
ILA	−0,571	0,810*†	0,024	0,881**†	0,257	0,262
PLA	−0,524	0,881**†	0,143	0,619	−0,029	0,548
4HPLA	−0,357	0,881**†	0,738	0,833*†	−0,086	0,310
Trp	−0,476	−0,167	−0,214	0,524	0,600	−0,429
Phe	−0,262	0,048	−0,333	0,429	0,086	−0,024
Tyr	−0,191	0,143	−0,119	0,238	−0,086	−0,429
PPyA	−0,357	0,833*†	0,071	0,667	0,071	0,191
4HPPyA	−0,595	0,857*†	−0,595	0,691	−0,143	−0,659

Spearman's correlation r values, *$P < 0.05$, **$P < 0.01$, corrected P values: †$q < 0.05$.

of EcN impose a low genetic burden on the host cell (Zainuddin et al. 2019). In engineered probiotics, it is advantageous to reduce a vector's genetic and metabolic burden to mitigate selective pressure against the synthetic functions and facilitate proliferation and colonization of the strain (Riglar and Silver 2018). The constructed strain described in this study reached a similar maximal growth rate to its unmodified counterpart, while further analysis is needed to identify the mutation rate of the construct.

Escherichia coli has been described previously as both an ILA and IPyA producer (Smith and Macfarlane 1996). Our results confirmed the ability of EcN to produce IPyA, but we did not detect a substantial ILA production. Aromatic metabolite production depends on environmental conditions and substrate availability (Smith and Macfarlane 1996), which might explain this divergence. Additionally, no *E. coli* dehydrogenase involved in the conversion of IPyA to ILA is present in the current literature, although *E.coli* contains a vast amount of this family of enzymes (Keseler et al. 2011). We propose that the occasional ILA production in *E. coli* observed by others could result from non-specific conversion of the aPyAs.

Several enzymes, including AspC and TyrB, have been shown or suspected to generate pyruvic acids from amino acids in *E.coli* (Mavrides and Orr 1975, Romasi and Lee 2013). Nevertheless, the lack of detection of more than traces of IPyA in our *in vitro* tests may reflect that it is a labile compound. IPyA and the other aPyAs may thus degrade soon after production, or enzymatic preference towards other substrates than the parental aromatic amino acids may prevent the generation of these intermediates. Most enzymes exhibit some level of infidelity in recognizing potential substrates (Khersonsky and Tawfik 2010). In *E.coli*, 37% of its enzymes are estimated to be promiscuous (Nam et al. 2012). In our construct, Aldh converts aPyAs into ILA, PLA, and 4HPLA. Regarding the high production of aLAs, whereas, no comparable concentrations of aPyAs have been detected in the EcN *aldh* cultures, we speculate that aLAs in the EcN *aldh* cultures might prompt aPyA synthesis through a positive feedback regulation loop.

A recent report reveals that Aldh from *B. longum* subsp. *longum* favours tryptophan degradation over the other aromatic amino acids (Laursen et al. 2020). In line with this, despite a much higher concentration of phenylalanine and tyrosine in the media, tryptophan-to-ILA conversion by EcN *aldh* was more potent than the conversions of phenylalanine and tyrosine. Such enzymatic preferences appear to be species-specific. Characterization of a similar pathway, encoded by the fldABC operon in *Clostridium sporogenes*, showed a preference for phenylalanine degradation (Dodd et al. 2017). The evolution of intestinal bacteria's aromatic amino acid degradation pathways to exhibit different preferences on substrates may depict the adaptation of each species to the amino acid pool offered by the host.

Colonization of streptomycin-resistant EcN strains in a streptomycin-treated mouse model reached comparable levels of the EcN *aldh* and the control (Fig. 2), with around 10E9 bacteria per gram of gut content establishing themselves in the cecum and colon of the mice. The production of ILA significantly increased upon EcN *aldh* administration (Fig. 3A). As the *aldh* gene is expressed in a continuous fashion, its products were present from day one after the AMT administration. Furthermore, the difference in ILA concentration in the intestinal compartments is substantial between the two groups of mice. The small increase of ILA observed in the EcN-treated mice may be a result of the gradual adaptation to the streptomycin-driven conditions (Ng et al. 2019) and/or incorporation of EcN.

Intestinal ILA levels were highest in the cecum, consistent with EcN that mainly resides in the cecum and colon of the mammalian intestine (Conway et al. 2004). In addition to ILA, also PLA and 4HPLA were present in considerable amounts in the feces and the gut of EcN *aldh* mice. Likewise to ILA dynamics, these aLAs increased over time in the EcN group, although their levels remained significantly lower than in the EcN *aldh* group, thus the observed changes could be attributed to adaptation dynamics due to streptomycin.

Of note, changes were observed in the systemic circulation. ILA serum almost doubled in the strep treated animals after EcN *aldh* colonization, while it did not increase in response to EcN (Fig. 4A). Thus far, it has been hard to detect observable differences or trends in the systemic circulation elicited by a single AMT (Bai et al. 2020, Yan et al. 2021). Hence, although further experiments are need to confirm our finding, the ILA-producing EcN *aldh* may be a promising agent for microbiome interventions.

The correlation between EcN *aldh* in the intestinal tract and ILA and 4HPLA concentration (Table 1) underlines the probability of the contribution of the strain to the production of the metabolites. In addition, the observed EcN *aldh*-to-ILA relationship could be advantageous for future studies, especially in animal disease models. A linear relationship implies that genetic manipulation of *aldh* expression, which quickly shows *in vitro*, will probably be easily expressed *in vivo*. Altogether, our strain's performance shows an AMT that has prospects for testing on a disease model.

We propose that the beneficial effects of ILA in combination with the probiotic capacity of EcN may result in a potent AMT strain. Based on ILA associations with healthy phenotypes, its putative applications range from treating necrotizing enterocolitis (Ehrlich et al. 2020, Meng et al. 2020) and boosting immune system maturation in infants (Huang et al. 2021). Thus, EcN *aldh* is

suitable to proceed into pre-clinical studies to assess its therapeutic potential. It should be noted that many options exist for further improvement of the strain. Particularly in association with its putative use as an AMT, curation of the two cryptic plasmids, deletion of all resistance genes, and addition of an inducible killing switch to ensure containment are needed before claiming a strain that may proceed into toxicity assessment and clinical trials.

Conclusion

We have presented the construction and *in vivo* evaluation of an engineered probiotic strain to enhance ILA production in the gut. EcN *aldh* is a promising candidate for functions such as boosting non-breastfed infants' immune system development and preventing necrotizing enterocolitis. Yet, further studies are needed to support the beneficial effect the strain as a future AMT.

Acknowledgements

The authors thank Katja Ann Kristensen for excellent technical assistance, and Priscila Guerra for valuable practical help with animal experiments.

Supplementary data

Supplementary data are available at *FEMSLE* online.

Conflict of interest. None declared.

Funding

This work was supported by the Novo Nordisk Foundation under NFF grant number: NNF10CC1016517 and The Novo Nordisk Foundation, Challenge programme, CaMiT under grant agreement: NNF17CO0028232.

References

Armetta J, Schantz-Klausen M, Shepelin D *et al. Escherichia coli* promoters with consistent expression throughout the Murine gut. *ACS Synth Biol* 2021;**10**:3359–68. https://doi.org/10.1021/acssynbio.1c00325

Bai L, Gao M, Cheng X *et al.* Engineered butyrate-producing bacteria prevents high fat diet-induced obesity in mice. *Microb Cell Fact* 2020;**19**:94. https://doi.org/10.1186/s12934-020-01350-z

Benjamini Y, Hochberg Y. On the adaptive control of the false discovery rate in multiple testing with independent statistics. *J Educ Behav Stat* 2000;**25**:60–83. https://doi.org/10.3102/10769986025001060

Brandl MT, Lindow SE. Cloning and characterization of a locus encoding an indolepyruvate decarboxylase involved in indole-3-acetic acid synthesis in Erwinia herbicola. *Appl Environ Microbiol* 1996;**62**:4121–8. https://doi.org/10.1128/aem.62.11.4121-4128.1996

Cani PD. Microbiota and metabolites in metabolic diseases. *Nat Rev Endocrinol* 2019;**15**:69–70. https://doi.org/10.1038/s41574-018-0143-9

Cervantes-Barragan L, Chai JN, Tianero MD *et al.*. *Science* 2017;**357**:806–10.

Chevrette MG, Thomas CS, Hurley A *et al.* Microbiome composition modulates secondary metabolism in a multispecies bacterial community. *Proc Natl Acad Sci USA* 2022;**119**:e2212930119. https://doi.org/10.1073/pnas.2212930119

Clarke G, Stilling RM, Kennedy PJ *et al.* Minireview: gut microbiota: the neglected endocrine organ. *Mol Endocrinol* 2014;**28**:1221–38. https://doi.org/10.1210/me.2014-1108

Conlan JW, Bardy SL, KuoLee R *et al.* Ability of *Escherichia coli* O157:H7 isolates to colonize the intestinal tract of conventional adult CD1 mice is transient. *Can J Microbiol* 2001;**47**:91–95. https://doi.org/10.1139/w00-124

Conway T, Krogfelt KA, Cohen PS. The life of commensal *Escherichia coli* in the mammalian intestine. *EcoSal Plus* 2004;**1**. https://doi.org/10.1128/ecosalplus.8.3.1.2

Derrien M, Turroni F, Ventura M *et al.* Insights into endogenous *Bifidobacterium* species in the human gut microbiota during adulthood. *Trends Microbiol* 2022;**30**:940–7. https://doi.org/10.1016/j.tim.2022.04.004

Diaz Ricci JC, Hernández ME. Plasmid effects on *Escherichia coli* metabolism. *Crit Rev Biotechnol* 2000;**20**:79–108. https://doi.org/10.1080/07388550008984167

Dodd D, Spitzer MH, Van Treuren W *et al.* A gut bacterial pathway metabolizes aromatic amino acids into nine circulating metabolites. *Nature* 2017;**551**:648–52. https://doi.org/10.1038/nature24661

Ehrlich AM, Pacheco AR, Henrick BM *et al.* Indole-3-lactic acid associated with *Bifidobacterium*-dominated microbiota significantly decreases inflammation in intestinal epithelial cells. *BMC Microbiol* 2020;**20**:357. https://doi.org/10.1186/s12866-020-02023-y

Francino MP. Early development of the gut microbiota and immune health. *Pathogens* 2014;**3**:769–90. https://doi.org/10.3390/pathogens3030769

Green MR, Hughes H, Sambrook J *et al. Molecular Cloning: A Laboratory Manual*. **Vol. 1**, Cold Spring Harbor Laboratory Press, 2012.

Han S, Lu Y, Xie J *et al.* Probiotic gastrointestinal transit and colonization after oral administration: a long journey. *Front Cell Infect Microbiol* 2021;**11**:609722. https://doi.org/10.3389/fcimb.2021.609722

Hecht A, Glasgow J, Jaschke PR *et al.* Measurements of translation initiation from all 64 codons in *E. coli*. *Nucleic Acids Res* 2017;**45**:3615–26. https://doi.org/10.1093/nar/gkx070

Henrick BM, Rodriguez L, Lakshmikanth T *et al.* Bifidobacteria-mediated immune system imprinting early in life. *Cell* 2021;**184**:3884–98. e11. https://doi.org/10.1016/j.cell.2021.05.030

Huang W, Cho KY, Meng D *et al.* The impact of indole-3-lactic acid on immature intestinal innate immunity and development: a transcriptomic analysis. *Sci Rep* 2021;**11**:8088. https://doi.org/10.1038/s41598-021-87353-1

Kearney SM, Gibbons SM, Erdman SE *et al.* Orthogonal dietary niche enables reversible engraftment of a gut bacterial commensal. *Cell Rep* 2018;**24**:1842–51. https://doi.org/10.1016/j.celrep.2018.07.032

Keseler IM, Collado-Vides J, Santos-Zavaleta A *et al.* EcoCyc: a comprehensive database of *Escherichia coli* biology. *Nucleic Acids Res* 2011;**39**:D583–90. https://doi.org/10.1093/nar/gkq1143

Khersonsky O, Tawfik DS. Enzyme promiscuity: a mechanistic and evolutionary perspective. *Annu Rev Biochem* 2010;**79**:471–505. https://doi.org/10.1146/annurev-biochem-030409-143718

Kotula JW, Kerns SJ, Shaket LA *et al.* Programmable bacteria detect and record an environmental signal in the mammalian gut. *Proc Natl Acad Sci USA* 2014;**111**:4838–43. https://doi.org/10.1073/pnas.1321321111

Laursen MF, Sakanaka M, von Burg N *et al.* Breastmilk-promoted bifidobacteria produce aromatic lactic acids in the infant gut. *Biorxiv* 2020, https://doi.org/10.1101/2020.01.22.914994

Laursen MF, Sakanaka M, von Burg N *et al. Bifidobacterium* species associated with breastfeeding produce aromatic lactic acids in the infant gut. *Nat Microbiol* 2021;**6**:1367–82. https://doi.org/10.1038/s41564-021-00970-4

Lavelle A, Sokol H. Gut microbiota-derived metabolites as key actors in inflammatory bowel disease. *Nat Rev Gastroenterol Hepatol* 2020;**17**:223–37. https://doi.org/10.1038/s41575-019-0258-z

Lin-Chao S, Bremer H. Effect of the bacterial growth rate on replication control of plasmid pBR322 in *Escherichia coli*. *Mol Gen Genet* 1986;**203**:143–9. https://doi.org/10.1007/BF00330395

Liu Y, Hou Y, Wang G *et al.* Gut microbial metabolites of aromatic amino acids as signals in host-microbe interplay. *Trends Endocrinol Metab* 2020;**31**:818–34. https://doi.org/10.1016/j.tem.2020.02.012

Mandell DJ, Lajoie MJ, Mee MT *et al.* Biocontainment of genetically modified organisms by synthetic protein design. *Nature* 2015;**518**:55–60. https://doi.org/10.1038/nature14121

Mano Y, Nemoto K. The pathway of auxin biosynthesis in plants. *J Exp Bot* 2012;**63**:2853–72. https://doi.org/10.1093/jxb/ers091

Mavrides C, Orr W. Multispecific aspartate and aromatic amino acid aminotransferases in *Escherichia coli*. *J Biol Chem* 1975;**250**:4128–33. https://doi.org/10.1016/S0021-9258(19)41395-1

Meng D, Sommella E, Salviati E *et al.* Indole-3-lactic acid, a metabolite of tryptophan, secreted by *Bifidobacterium longum* subspecies infantis is anti-inflammatory in the immature intestine. *Pediatr Res* 2020;**88**:209–17. https://doi.org/10.1038/s41390-019-0740-x

Mimee M, Citorik RJ, Lu TK. Microbiome therapeutics—advances and challenges. *Adv Drug Deliv Rev* 2016;**105**:44–54. https://doi.org/10.1016/j.addr.2016.04.032

Nam H, Lewis NE, Lerman JA *et al.* Network context and selection in the evolution to enzyme specificity. *Science* 2012;**337**:1101–4. https://doi.org/10.1126/science.1216861

Ng KM, Aranda-Díaz A, Tropini C *et al.* Recovery of the gut microbiota after antibiotics depends on host diet, community context, and environmental reservoirs. *Cell Host Microbe* 2019;**26**:650–65. e4. https://doi.org/10.1016/j.chom.2019.10.011

Nielsen LN, Roager HM, Casas ME *et al.* Glyphosate has limited short-term effects on commensal bacterial community composition in the gut environment due to sufficient aromatic amino acid levels. *Environ Pollut* 2018;**233**:364–76. https://doi.org/10.1016/j.envpol.2017.10.016

Ou B, Yang Y, Tham WL *et al.* Genetic engineering of probiotic *Escherichia coli* Nissle 1917 for clinical application. *Appl Microbiol Biotechnol* 2016;**100**:8693–9. https://doi.org/10.1007/s00253-016-7829-5

Ozdemir T, Fedorec AJH, Danino T *et al.* Synthetic biology and engineered live biotherapeutics: toward increasing system complexity. *Cell Syst* 2018;**7**:5–16. https://doi.org/10.1016/j.cels.2018.06.008

Pedrolli DB, Ribeiro NV, Squizato PN Team AQA Unesp at iGEM 2017 *et al.*.. Engineering microbial living therapeutics: the synthetic biology toolbox. *Trends Biotechnol* 2019;**37**:100–15. https://doi.org/10.1016/j.tibtech.2018.09.005

Peredo-Lovillo A, Romero-Luna HE, Jiménez-Fernández M. Health promoting microbial metabolites produced by gut microbiota after prebiotics metabolism. *Food Res Int* 2020;**136**:109473. https://doi.org/10.1016/j.foodres.2020.109473

Piraner DI, Abedi MH, Moser BA *et al.* Tunable thermal bioswitches for in vivo control of microbial therapeutics. *Nat Chem Biol* 2017;**13**:75–80. https://doi.org/10.1038/nchembio.2233

Riglar DT, Silver PA. Engineering bacteria for diagnostic and therapeutic applications. *Nat Rev Microbiol* 2018;**16**:214–25. https://doi.org/10.1038/nrmicro.2017.172

Roager HM, Licht TR. Microbial tryptophan catabolites in health and disease. *Nat Commun* 2018;**9**:3294. https://doi.org/10.1038/s41467-018-05470-4

Romasi EF, Lee J. Development of indole-3-acetic acid-producing *Escherichia coli* by functional expression of IpdC, AspC, and Iad1. *J Microbiol Biotechnol* 2013;**23**:1726–36. https://doi.org/10.4014/jmb.1308.08082

Ruijter JM, Ramakers C, Hoogaars WMH *et al.* Amplification efficiency: linking baseline and bias in the analysis of quantitative PCR data. *Nucleic Acids Res* 2009;**37**:e45. https://doi.org/10.1093/nar/gkp045

Russell WR, Duncan SH, Scobbie L *et al.* Major phenylpropanoid-derived metabolites in the human gut can arise from microbial fermentation of protein. *Mol Nutr Food Res* 2013;**57**:523–35. https://doi.org/10.1002/mnfr.201200594

Rutsch A, Kantsjö JB, Ronchi F. The gut-brain axis: how microbiota and host inflammasome influence brain physiology and pathology. *Front Immunol* 2020;**11**:604179. https://doi.org/10.3389/fimmu.2020.604179

Ryan RM, Green J, Williams PJ *et al.* Bacterial delivery of a novel cytolysin to hypoxic areas of solid tumors. *Gene Ther* 2009;**16**:329–39. https://doi.org/10.1038/gt.2008.188

Sakurai T, Odamaki T, Xiao J-Z. Production of indole-3-lactic acid by bifidobacterium strains isolated fromHuman infants. *Microorganisms* 2019;**7**. https://doi.org/10.3390/microorganisms7090340

Salis HM. The ribosome binding site calculator. *Methods Enzymol* 2011;**498**:19–42. https://doi.org/10.1016/B978-0-12-385120-8.00002-4

Sardar P, Kempken F. Characterization of indole-3-pyruvic acid pathway-mediated biosynthesis of auxin in *Neurospora crassa*. *PLoS One* 2018;**13**:e0192293. https://doi.org/10.1371/journal.pone.0192293

Schröder NCH, Korša A, Wami H *et al.* Serial passage in an insect host indicates genetic stability of the human probiotic *Escherichia coli* Nissle 1917. *Evol Med Public Health* 2022;**10**:71–86. https://doi.org/10.1093/emph/eoac001

Sharma V, Smolin J, Nayak J *et al.* Mannose alters gut microbiome, prevents diet-induced obesity, and improves host metabolism. *Cell Rep* 2018;**24**:3087–98. https://doi.org/10.1016/j.celrep.2018.08.064

Shepherd ES, DeLoache WC, Pruss KM *et al.* An exclusive metabolic niche enables strain engraftment in the gut microbiota. *Nature* 2018;**557**:434–8. https://doi.org/10.1038/s41586-018-0092-4

Singh BP, Rateb ME, Rodriguez-Couto S *et al.* Editorial: microbial secondary metabolites: recent developments and technological challenges. *Front Microbiol* 2019;**10**:914. https://doi.org/10.3389/fmicb.2019.00914

Smith EA, Macfarlane GT. Enumeration of human colonic bacteria producing phenolic and indolic compounds: effects of pH, carbohydrate availability and retention time on dissimilatory aromatic amino acid metabolism. *J Appl Bacteriol* 1996;**81**:288–302. https://doi.org/10.1111/j.1365-2672.1996.tb04331.x

Sonnenborn U, Schulze J. . *Microb Ecol Health Disease* 2009;**21**:122–58.

Suez J, Elinav E. The path towards microbiome-based metabolite treatment. *Nat Microbiol* 2017;**2**:17075. https://doi.org/10.1038/nmicrobiol.2017.75

Thomas P, Sekhar AC, Upreti R *et al.* Optimization of single plate-serial dilution spotting (SP-SDS) with sample anchoring as an assured method for bacterial and yeast cfu enumeration and single colony isolation from diverse samples. *Biotechnol Rep* 2015;**8**:45–55. https://doi.org/10.1016/j.btre.2015.08.003

Wadolkowski EA, Laux DC, Cohen PS. Colonization of the streptomycin-treated mouse large intestine by a human fecal *Escherichia coli* strain: role of adhesion to mucosal receptors.

Infect Immun 1988;**56**:1036–43. https://doi.org/10.1128/iai.56.5.1036-1043.1988

Wang Z, Xiang L, Shao J *et al.* Effects of the presence of ColE1 plasmid DNA in *Escherichia coli* on the host cell metabolism. *Microb Cell Fact* 2006;**5**:34. https://doi.org/10.1186/1475-2859-5-34

Wilck N, Matus MG, Kearney SM *et al.* Salt-responsive gut commensal modulates TH17 axis and disease. *Nature* 2017;**551**:585–9. https://doi.org/10.1038/nature24628

Wong CB, Tanaka A, Kuhara T *et al.* Potential effects of indole-3-lactic acid, a metabolite of Human bifidobacteria, on NGF-induced neurite outgrowth in PC12 cells. *Microorganisms* 2020;**8**. https://doi.org/10.3390/microorganisms8030398

Xiao Y, Zhai Q, Zhang H *et al.* Gut colonization mechanisms of lactobacillus and bifidobacterium: an argument for personalized designs. *Annu Rev Food Sci Technol* 2021;**12**:213–33. https://doi.org/10.1146/annurev-food-061120-014739

Yan X, Liu X-Y, Zhang D *et al.* Construction of a sustainable 3-hydroxybutyrate-producing probiotic *Escherichia coli* for treatment of colitis. *Cel Mol Immunol* 2021;**18**:2344–57. https://doi.org/10.1038/s41423-021-00760-2

Zainuddin HS, Bai Y, Mansell TJ. CRISPR-based curing and analysis of metabolic burden of cryptic plasmids in *Escherichia coli* Nissle 1917. *Eng Life Sci* 2019;**19**:478–85. https://doi.org/10.1002/elsc.201900003

Zhou Q, Xie Z, Wu D *et al.* The effect of indole-3-lactic acid from lactiplantibacillus plantarum ZJ316 on Human intestinal microbiota In vitro. *Foods* 2022;**11**:3302. https://doi.org/10.3390/foods11203302

Zhu W, Stevens AP, Dettmer K *et al.* Quantitative profiling of tryptophan metabolites in serum, urine, and cell culture supernatants by liquid chromatography-tandem mass spectrometry. *Anal Bioanal Chem* 2011;**401**:3249–61. https://doi.org/10.1007/s00216-011-5436-y

Zmora N, Zilberman-Schapira G, Suez J *et al.* Personalized gut mucosal colonization resistance to empiric probiotics is associated with unique host and microbiome features. *Cell* 2018;**174**:1388–405. https://doi.org/10.1016/j.cell.2018.08.041

Conway T, Krogfelt KA, Cohen PS. The life of commensal *Escherichia coli* in the mammalian intestine. *EcoSal Plus* 2004;**1**, 1. https://doi.org/10.1128/ecosalplus.8.3.1.2

Ehrlich AM, Pacheco AR, Henrick BM *et al.* 2020. Indole-3-lactic acid associated with bifidobacterium-dominated microbiota significantly decreases inflammation in intestinal epithelial cells. *BMC Microbiol* **20**:357. https://doi.org/10.1186/s12866-020-02023-y

Zmora N, Zilberman-Schapira G, Suez J *et al.* Personalized gut mucosal colonization resistance to empiric probiotics is associated with unique host and microbiome features. *Cell* 2018;**174**:1388–405. https://doi.org/10.1016/j.cell.2018.08.041